Expression of Human Foamy Virus Is Differentially Regulated during Development in Transgenic Mice

Adriano Aguzzi,[1,*] Katrin Bothe,[2] Ingrid Anhauser,[1] Ivan Horak,[2] Axel Rethwilm,[2] Erwin F. Wagner[1]

The human foamy virus (HFV) is a recently characterized member of the spumavirus family. Although no diseases have been unequivocally associated with HFV infection, expression of HFV regulatory genes in transgenic mice induces a characteristic acute neurodegenerative disease and a myopathy. To better characterize the sequence of events leading to disease, and to gain a better understanding of the underlying pathogenetic mechanisms, we have analyzed in detail the transgene expression pattern during development. Transcription of a construct containing all regulatory elements and ancillary genes of HFV was analyzed by in situ hybridization and was shown to occur in two distinct phases. At midgestation, low but widespread expression was first detected in cells of extraembryonic tissues. Later, various tissues originating from embryonic mesoderm, neuroectoderm, and neural crest transcribed the transgene at moderate levels. However, expression decreased dramatically during late gestation and was suppressed shortly after birth. After a latency period of up to 5 weeks, transcription of the transgene resumed in single cells distributed irregularly in the central nervous system and in the skeletal muscle. By the age of 8 weeks, an increasing number of cells displayed much higher expression levels than in embryonic life and eventually underwent severe degenerative changes. These findings demonstrate that HFV transgene expression is differentially regulated in development and that HFV cytotoxicity may be dose-dependent. Such biphasic pattern of expression differs from that of murine retroviruses and may be explained by the specificity of HFV regulatory elements in combination with cellular factors. Future studies of this model system should, therefore, provide novel insights in the mechanisms controlling retroviral latency.

Received November 18, 1991; revised January 2, 1992

Although in vivo model systems and studies with cultured cells have contributed a large body of information on gene expression, tissue tropism, and virulence of human retroviruses (reviewed by Gallo and Wong-Staal, 1990), little is known about these parameters in the case of prenatally acquired infection. Studies of the control of human retroviral gene expression during prenatal development are important because they may lead, for example, to an understanding of the high frequency of vertical transmission of the human immunodeficiency virus, HIV (European Collaborative Study 1991; Lyman et al., 1990; Joshi et al., 1990), for which atypical infection routes and pathologies specific to embryonic infection have been identified (Lewis et al., 1990, Giangaspero et al., 1989). Another poorly understood aspect of gene expression, which is also of clinical significance, is the control that occurs during the latency period that follows retroviral infection. Detailed analyses of these phenomena have been hampered by the complex genomic organization of the known human retroviruses and by the lack of suitable animal model systems.

While most studies of retroviral gene expression have been conducted with human T-cell lymphotropic viruses (HTLV) and HIV, we have focused on the specific properties of the human foamy virus (HFV), a recently characterized member of the family of spumaviruses. Like HTLV and HIV, HFV contains a complex genome. In addition to the structural retroviral genes *gag, pol,* and *env,* HFV includes three open reading frames in its 3'-terminal region; these are termed *bel-1, bel-2,* and *bel-3* (Flügel et al., 1987). Three additional open reading frames, *bet, bes,* and *beo,* may be generated by alternative splicing (Muranyi and Flügel, 1991;

[1]Research Institute of Molecular Pathology (I.M.P.), Dr. Bohr Gasse 7, A-1030 Vienna, Austria.
[2]Institute of Virology and Immunobiology, University of Würzburg, Versbacherstrasse 7, D-W-8700 Würzburg, Germany.
*To whom correspondence should be addressed.

1043-4674/92/0403-0007$5.00/0

KEY WORDS: human foamy virus/transgenic mice/mouse embryogenesis/in situ hybridization

Löchelt et al., 1991). The *bel-1* gene product was shown to act as a trans-activating transcription factor (Rethwilm et al., 1990, 1991), but it has limited structural homology to the Tat trans-activator of HIV-2 and the molecular basis of its action remains poorly understood. No function has yet been assigned to the proteins encoded by the other accessory open reading frames.

Human foamy virus has been isolated from patients with disparate conditions (Achong et al., 1971, Cameron et al., 1978). Despite the geographically clustered prevalence of HFV (Muller et al., 1980) and a possible epidemiological link with de Quervain's thyroiditis (Stancek et al., 1975; Werner and Gelderblom, 1979), it has not been convincingly demonstrated that HFV is the causative agent of any human disease, and indeed HFV has often been considered to be a benign retrovirus (Coffin, 1990).

Although some important properties of HFV have been elucidated, it has not yet been possible to directly identify the tissue-specific pattern of infectibility and expression of HFV. These considerations prompted us to search for an animal model system, and we decided to introduce HFV genes into the germ line of mice (Bothe et al., 1991). Transgenic mice carrying genes and autologous regulatory elements of human retroviruses have developed pathologies similar to those encountered in natural infections, thereby providing powerful model systems (Hinrichs et al., 1987; Leonard et al., 1988; Nerenberg and Wiley 1989). Such systems are easily accessible to morphological and molecular analysis and, since they may allow prenatal expression, can also be used to study vertical transmission.

We found previously that transgenic mice expressing HFV genes develop a characteristic neurodegenerative and myopathic disorder (Bothe et al., 1991). These studies provided the first experimental evidence of a specific pathology associated with the expression of these genes. It seemed that one or more HFV regulatory genes may be directly cytotoxic, since we observed a close correlation between gene expression and tissue damage in both transgenic mice containing essentially the whole HFV genome (HFV_{Af}) and in mice expressing a mutated construct (named Δgpe) in which only the ancillary genes are intact.

To further establish the causal relation between the expression of this transgene and the development of HFV-induced disease in Δgpe transgenic mice, we examined the tissues to determine which ones expressed the transgene at the different developmental stages, and to find out whether such expression always leads to cell degeneration. Here, we show that a moderate amount of transcriptional activity of the transgene is detectable during embryonic life in several tissues, but that such expression is transient and not accompanied by pathological changes. Expression resumes in adult mice and is found at high levels only after a long latency period in a restricted range of tissues.

RESULTS

Expression of the HFV Transgene Is Turned on at E8.5 in Extraembryonic Tissues and Later in Embryonic Tissues

The earliest developmental time point at which HFV transgenic embryos were collected and analyzed was embryonic day 8.5 (E8.5). Mouse embryos of this age show 8 to 14 somites and several recognizable organ rudiments. The morphology of HFV transgenic embryos was in good agreement with their gestational age (Theiler, 1989) as studied by conventional histology on serial paraffin sections. In particular, the neural groove showed normal differentiation and was closed in the thoracic portion. In situ hybridization analyses were performed on selected sections with a *bel* RNA probe complementary to sequences shared by all known HFV transcripts (Fig. 1). HFV expression in embryonic tissues was not generally activated at this developmental stage. Very low levels of transgenic RNA were detected only in the mesenchymal cells of the cranial somites (data not shown). In the extraembryonic structures, a signal of moderate intensity was recognizable

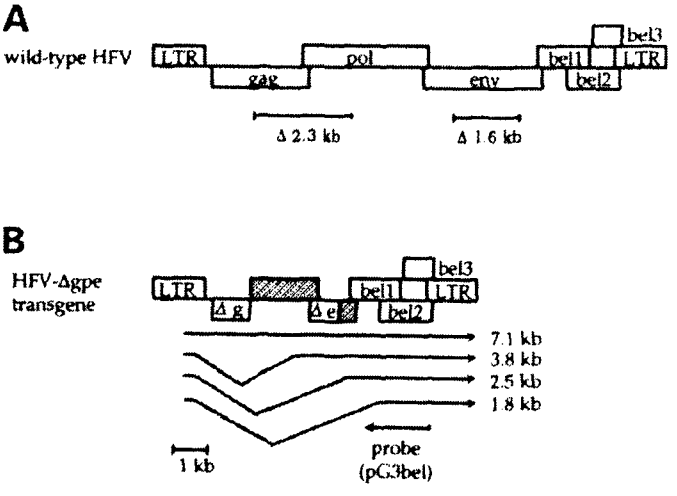

Figure 1. Organization of the HFV genome and the Δgpe construct.

(**A**) In the HFV genome, multispliced mRNA species may allow for translation of three additional compound gene products, from the *bet*, *bes*, and *beo* genes, which have been omitted in the figure. In the microinjected fragment, 2.3 and 1.6 kb have been deleted from the *gag*- *pool* and *env* domains, respectively, as indicated by horizontal bars. (**B**) Structure of the Δgpe construct used to generate transgenic mice and expected size of the major transcripts. This construct gives rise to a family of spliced transcripts (1.8 to 2.5 kb) allowing translation of the *bel* reading frames. The hatched pattern in the carboxyl-terminal portions of *pol* and *env* indicates their translation is ablated by the introduced deletions. However, truncated forms of *gag* and *env* (Δg and Δe) may be generated from the 7.1-kb genomic and the 3.8-kb subgenomic transcripts.

in cells of the amnion (Fig. 2), whereas the allantois and visceral and parietal yolk sac were negative. In embryos of 11.5 days and older, transgene expression started to increase to discrete levels in several organ systems, as described in the following sections.

Expression in the Developing Nervous System

Because of the neurological symptoms observed in adult animals, we paid particular attention to expression of the HFV transgene in the developing nervous system. The autoradiographic signal of the neuroectoderm at E8.5 did not exceed background, and the first neuroectodermal cells containing transgenic mRNA were detected in the neural tubes of E11.5 embryos. At this developmental stage and at all further time points, HFV expression was confined to migratory differentiating neuroectodermal cells and was undetectable in the germinal layers. For instance, in the forebrain anlage of E11.5 embryos, 3 to 4 days before differentiation of the primary cortex and even before the appearance of a distinct mantle zone, a signal of moderate intensity was present only in the cells located most peripherally, whereas all periventricular cells were negative (Fig. 3, a and b). In the developing olfactory bulb of embryos aged 13.5 and 14.5 days, a distinct hybridization signal was discernible only in those neural cells that had already migrated to the primary cortex (Fig. 3, c and d).

Starting at E13.5, increasing levels of expression were seen in the neural crest and in several tissues developing from this structure, most prominently in the dorsal root ganglia (Fig. 3, e and f). Expression in the dorsal root ganglia and in the intracranial sensory ganglia continued to increase until E16.5. The distribution of expressing cells in the developing spinal cord was similar to that observed in the brain: moderate amounts of HFV mRNA were present in the peripheral parts of the mantle layer, while the ventricular zone and the roof and floor plates of the neural tube were completely devoid of signal (Fig. 3, g and h). The signal was confined to large cells with round pale nuclei and lightly basophilic cytoplasm representing differen-

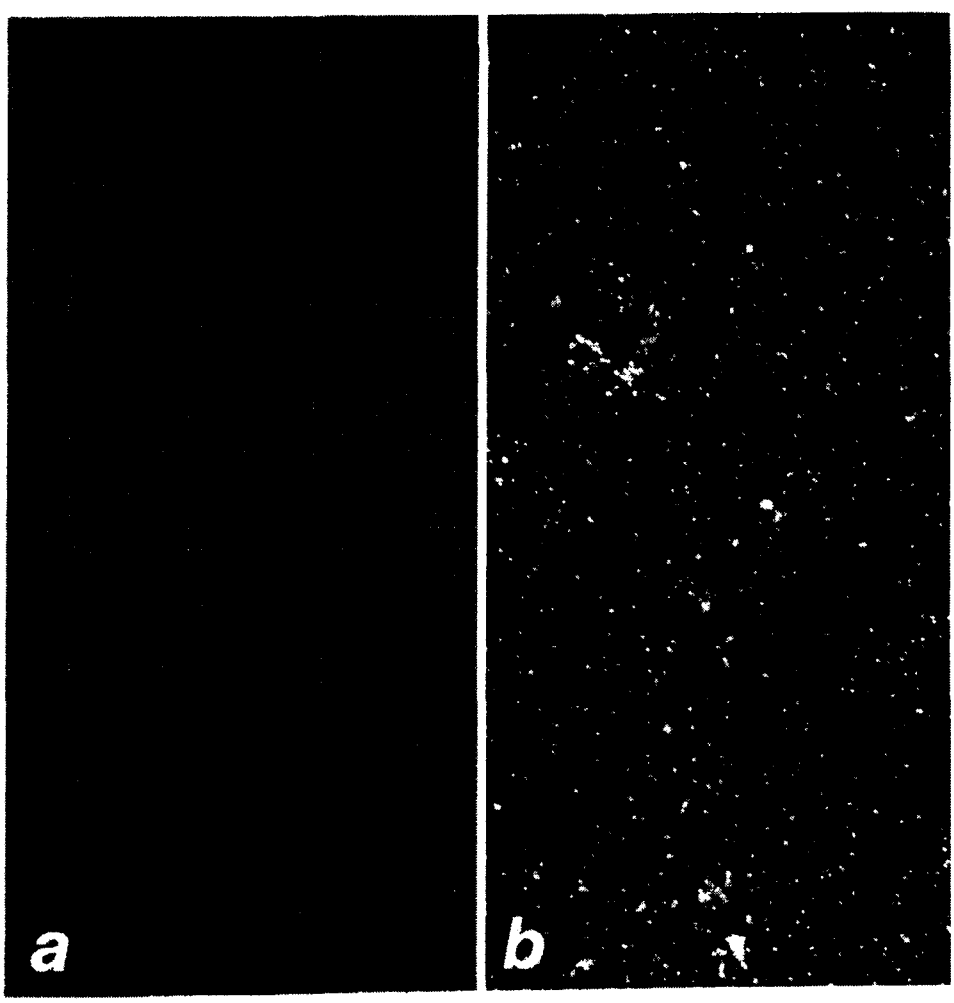

Figure 2. Expression of HFV in the amnion of an embryo aged 8.5 days (E8.5).

(**a**) Differential interference contrast. (**b**) Dark field (×200). At this stage only a few cells belonging to the amnion have started to transcribe low amounts of HFV genes (arrowheads).

THE NEW BIOLOGIST. Vol. 4, No. 3 (March 1992: 225-237)

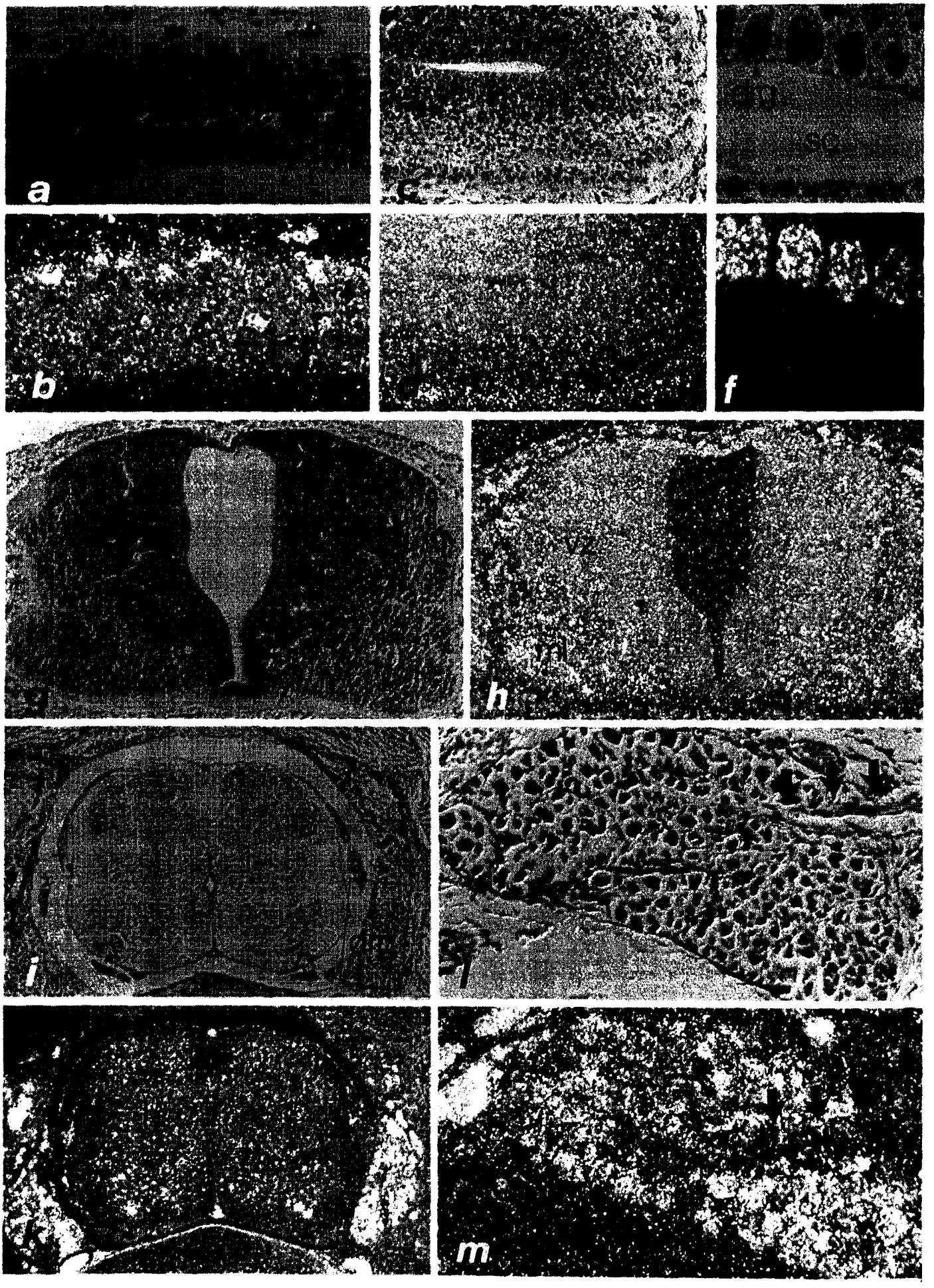

tiating neurons. Again, development of these embryos was normal. Prominent apoptosis was ongoing in several regions of the CNS and in the dorsal root ganglia at E13.5 to E14.5, as judged by the presence of numerous pyknotic cells, but the rates of apoptosis did not exceed those seen in normal time-matched control embryos.

The levels of transcription in cells of the nervous system at late gestation (E16.5 to birth) were generally much lower than at earlier time points. In the CNS, a prominent signal was localized in the facial nucleus and in the posterior hypothalamic area, and weaker hybridization was displayed by the cells in the tegmental neuroepithelium and by neurons in the pons varolii (data not shown). Low levels of expression were present also in the paravertebrally located sympathetic ganglia. In the spinal cord, development of columns and projection tracts proceeded normally until birth. The radial gradient of HFV expression detected at earlier time points in the neural tube was no longer discernible at this stage. High levels of expression were seen in a minor proportion of single motor neurons in the anterior columns (Fig. 3, i and k). In newborn mice the strongest signal was clearly located in the sensory neurons of the cranial and dorsal root ganglia (Fig. 3, i to m). Again, no obvious signs of enhanced cell degeneration were present. High-power micrographs of the sensory ganglia showed that only differentiated cells with obvious neuronal morphology expressed HFV, while satellite and Schwann cells as well as undifferentiated smaller neuroblastic cells did not contain transgenic mRNA (Fig. 3, l and m).

Expression in Cells of Mesodermal Origin and in Other Tissues

In contrast to our observations in adult mice, expression of the transgene in HFV embryos was not restricted to neuroectodermal and myogenic tissues but was also present in several other tissues. The majority of mesodermal cells in the region of the cardiac primordium already expressed significant amounts of the transgene at E11.5 (Fig. 4, a and b). At later time points (E13.5 and E14.5) it became apparent that transgenic mRNA was present in spindle-shaped cells belonging to the myocardium and also in pericardial fibroblasts (Fig. 4, c and d), but the number of expressing cells gradually decreased. At day 16.5 of gestation the pericardium was devoid of signal and myocardial expression was detected only in three out of eight embryos, where it was limited to very few cells located at the left atrio-ventricular junction and in the subendocardial layer of the left ventricle (Fig. 4, e and f). The topography of these cells suggests that they may constitute parts of the specialized myocardial excitation conduction system. Additionally, a strong signal was identified in cells at the aortico-pulmonary septation and in the pulmonary trunk (Fig. 4g). Cells situated in analogous locations are derived from the neural crest in chicken-quail chimaeras (Kirby et al., 1983).

A modest transgenic signal was always found at E16.5 and in newborn mice in a bilateral stream of cells located between the genital anlage and the vertebral column (Fig. 5, a to d). On serial sagittal and transversal sections of the lower abdomen and of the pelvis we identified these cells as neuroblasts of the autonomous nervous system. These cells originate from the neural crest and migrate during late organogenesis to the colon sigmoideum and rectum, where they eventually colonize the myenteric and submucosal plexus.

A number of structures originating from different germ layers displayed hybridization signals of various intensities between E13.5 and E16.5, including the posterior part of the pituitary gland rudiment (Fig. 5, e and f), a substantial proportion of cells in the base of the tongue identified as skeletal myoblasts (not shown), and groups of cells surrounding the hypopharynx and the esophagus (Fig. 5, g and h). Very low levels of expression were seen in the ganglion cell layer of the retina but not in the photoreceptor layer (not shown).

Figure 3. Expression of the transgene in developing neuroectodermal structures.

(**a** and **b**) Neuroepithelium of the telencephalic anlage at E11.5. The laminar pattern characteristic of the mature cortex is not yet discernible at this stage of development but only the external cells at more advanced stages of differentiation (arrows) express the transgene. (**c** and **d**) Olfactory bulb (E16.5). The ventricular zone containing neuroblastic precursors does not express transgenic RNA but a significant signal is identifiable in the differentiated olfactory epithelium (arrowheads). (**e** and **f**) Paramedian longitudinal section, E13.5. The spinal cord (sc) has produced vast amounts of projection fibers. The few cells embedded in this area and the ependymal cells visible at the bottom of the photograph do not express the transgene but expression is present in the dorsal root ganglia (drg). (**g** and **h**) Ventrolateral aspect of the thoracic spinal cord (E13.5). In analogy to the forebrain, the signal is concentrated on the more differentiated cells of the mantle layer (ml) while the grain counts on the ventricular zone (vz), despite its higher cellularity, hardly exceed background values. (**i** and **k**). Cross section through the spine of a newborn mouse. High levels of expression in the dorsal root ganglia (drg) and moderate expression in the spinal cord. Single motor neurons in the anterior columns (open arrowheads) express higher amounts of transgene. No expression in the dorsal roots, the meninges, and the surrounding non-neuroectodermal tissues. (**l** and **m**) The dorsal root ganglion in g and h shown at higher magnification. Note that the signal is present only in the differentiated sensory neurons, nor in the satellite cells nor in the Schwann cells (arrows).

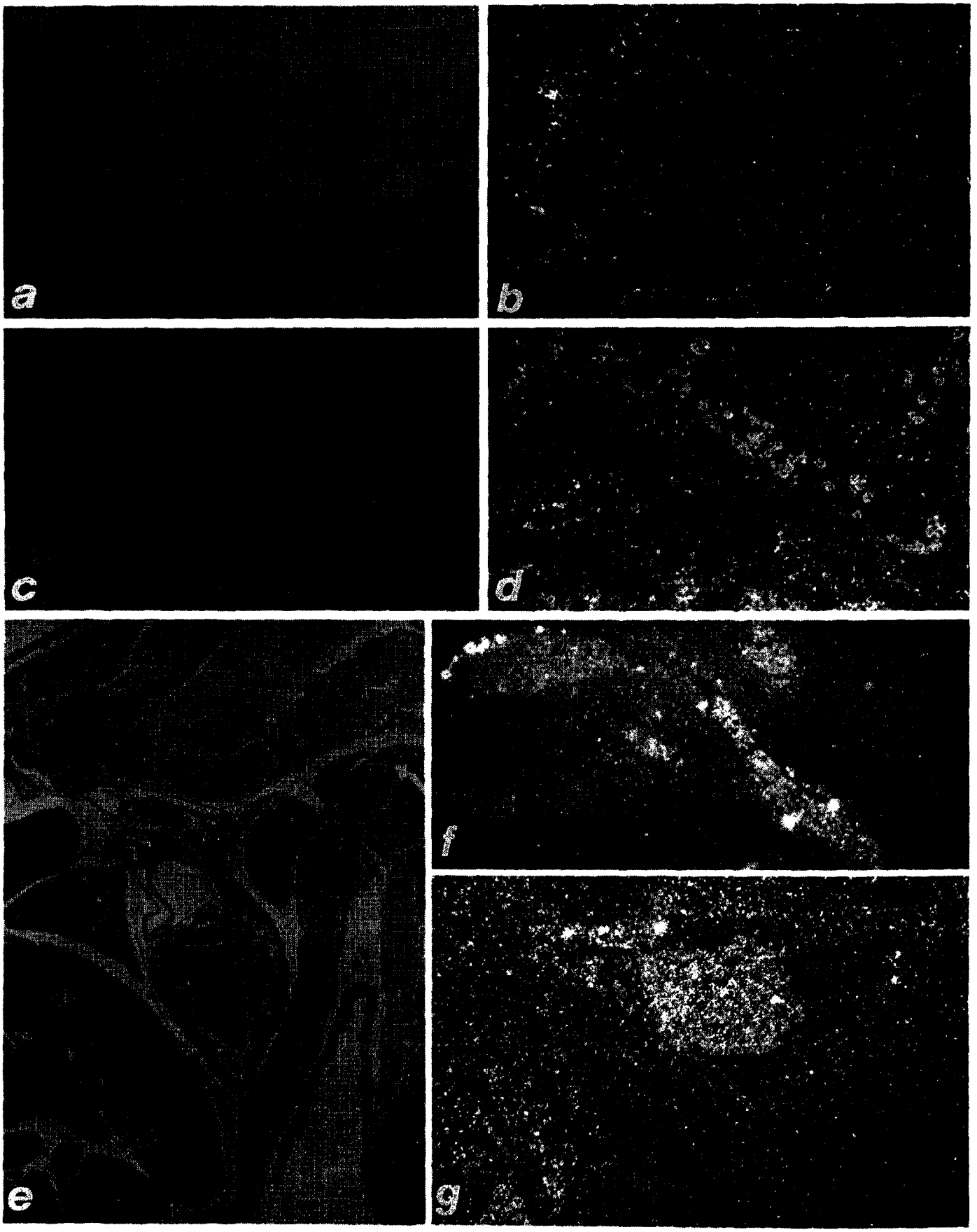
a
b
c
d
e
f
g

No signal was detected in the cells of the meningeal coverings. Endothelia were devoid of signal at all stages of development.

Activation of HFV Expression During Postnatal Life

In early postnatal life, expression of the HFV transgene was largely reduced or abolished in structures that had displayed a positive hybridization signal during intrauterine development. For example, no expression was seen in the pericardium and myocardium after birth. Also, in contrast to embryonic stages, the sinu-atrial and atrioventricular nodes and the rest of the conduction system of the heart did not show any expression. At postnatal day 21 and later, no expression and no tissue damage could be discerned in tissues of the peripheral nervous system, such as dorsal root ganglia and parasympathetic ganglia.

Despite the general lack of transcription described above, expression was resumed in the CNS after a latency phase of 3 to 5 weeks. At 3 weeks of age, most brain cells did not express detectable amounts of transgenic RNA, but a few scattered cells in the hippocampus (sector CA3) and in the cortex showed very high levels of expression. The number of these cells rapidly increased: at 5 weeks of age a substantial proportion of cortical neurons expressed the transgene (Fig. 6, a and b). The levels of expression in these cells were much higher than those attained in embryonic tissues. Additionally, small numbers of single cells ($< 1\%$) started to show very high levels of expression in the retina (not shown), in the paravertebral adipose tissue (Fig. 6, c and d), and the spinal cord. The number of spinal neurons resuming HFV expression was much lower than in the brain (Fig. 6e). The spinal cord of older HFV transgenic mice (12 week) showed a severe pathology of the white matter, which is more likely to result from degeneration of projecting cerebral neurons than from local toxic effects (Fig. 6e). A pattern similar to that observed in the brain developed in smooth muscle cells, particularly of the gastrointestinal tract, and in the skeletal striated musculature, where an increasing number of muscle fibers resumed expression of the HFV transgene after the third postnatal week (Fig. 6, f and g).

The high levels of HFV transgene expression documented in the tissues described above resulted in toxic effects in brain and striated muscle cells and, indeed, the oldest animals examined showed large areas of severe degeneration in the CNS and in the striated muscles. Consequently, total levels of transgene expression decreased again in these tissues because of a reduction in the number of cells expressing HFV mRNA (Fig. 7). No correlation between the severity of these findings and gene dosage could be observed in mice derived from transgenic founders with varying numbers of integrated copies, and HFV RNA levels were comparable in heterozygous and homozygous transgenic siblings (Fig. 7). Clinically, these mice suffered from a progressive neurological disease consisting of ataxia, spastic tetraparesis, and blindness, which eventually led to wasting and death. The course of this disease and its histopathological features have been documented (Bothe et al., 1991).

DISCUSSION

Biphasic Character of HVF Expression

Transcription of the transgene was detected long before the appearance of any histological or clinical sign of disease and was found to be extensively modulated during development. Two peaks of transcriptional activity during embryonic and postnatal life were detected (Fig. 8). In the first phase, expression was restricted to the amnion at embryonic day 8.5, but it soon extended to a suprisingly broad range of tissues of ectodermal and mesodermal origin. These structures contained cells uniformly expressing HFV at low or moderate levels. However, perinatally only subpopulations of neurons in the CNS and in the dorsal root ganglia were found to transcribe the transgene, and at 3 weeks of age expression was undetectable. Since no reduction in the number of neurons was detected in the dorsal root ganglia or in the spinal cord, degeneration of cells expressing HFV genes is unlikely to account for this finding. Instead, it seems that expression is downregulated in these tissues during late gestation and after birth.

After a latency period of several weeks, a different pattern emerged. In young adult mice an increasing number of cells in the CNS, the adipose tissue, and the smooth and striated muscles accumulated transgenic mRNA. The levels of transcriptional activity in these

Figure 4. Expression of the HFV transgene in the developing heart.

(**a** and **b**) Cardiac primordium (E8.5). Several mesenchymal cells express low to moderate amounts of the transgene (arrowheads). It is not possible at this stage to differentiate pericardial and epicardial precursors from heart muscle cells. (**c** and **d**) Heart anlage: region of the right atrium (E13.5). Myoblasts and elongated mesothelial cells forming the pericard (Pc) are now discernible. Pf, peri-epicardial folds (indicated by arrows). The arrowheads label positive cell clusters. (**e**) Thoracic cavity of a E16.5 embryo. Ht, heart; Sc, spinal cord; Lu, lung; Li, liver; Thy, thymus. (**f** and **g**) Details from the regions shown in boxes in e. Clusters of cells displaying a prominent signal by in situ hybridization in the pulmonary trunk and pulmonary arteries (f) as well as the atrioventricular node and cells in the wall of the left ventricle tentatively identified as the bundle of His (g).

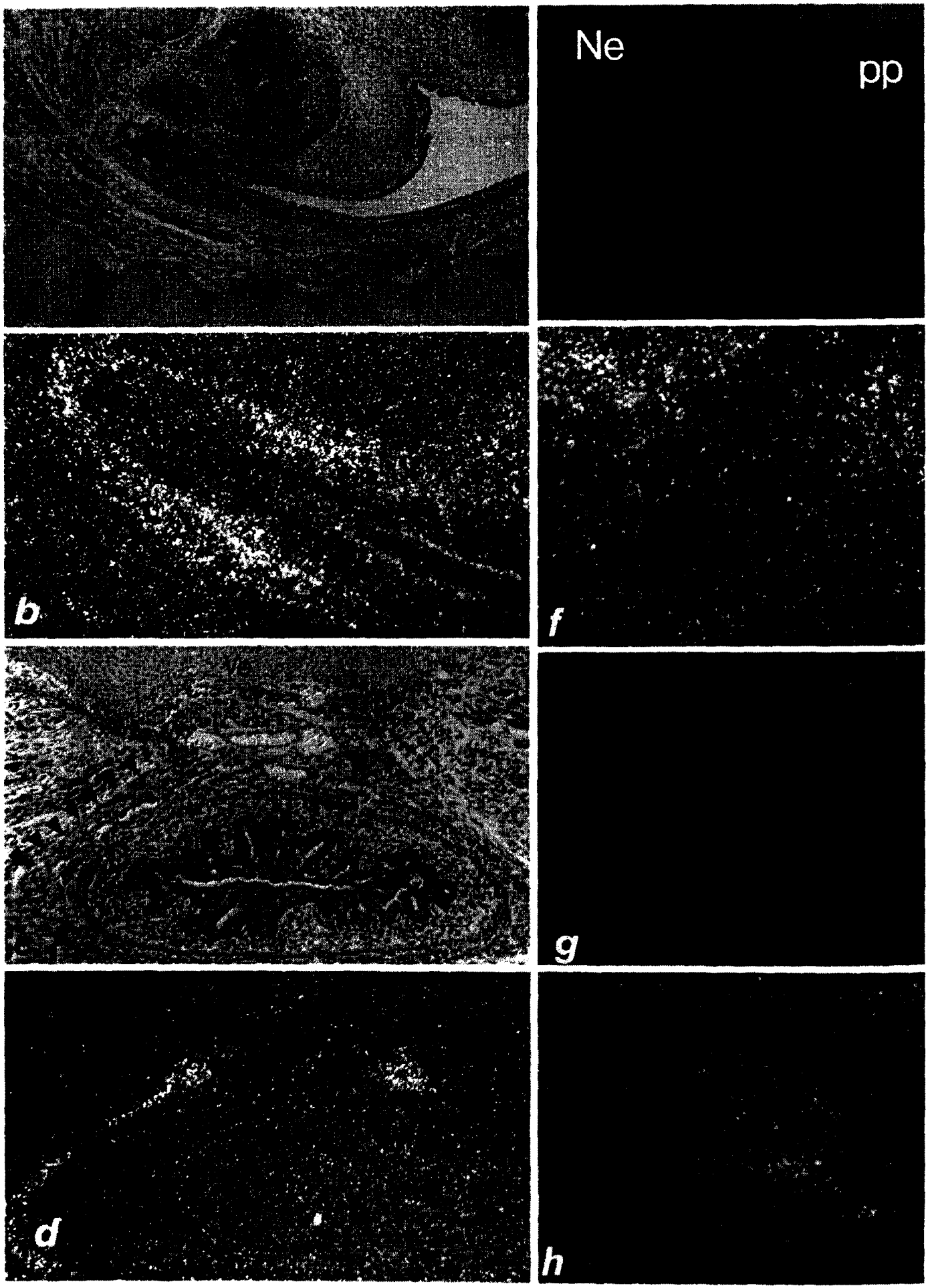
Ne
pp
b
f
g
d
h

cells were much higher than those reached during embryogenesis. In the CNS and striated musculature sustained expression was followed by cell degeneration.

The Embryonic and Adult Phases of Expression Differ in the Distribution of Cells Transcribing the Transgene

When transgenic mice of various ages were compared, it became apparent that the embryonic and adult phases of expression differed not only in the respective levels of transcriptional activity, but also with regard to the distribution of positive cells. Although the vast majority of cells in permissive tissues expressed comparable amounts of transgenic mRNA during embryonic development, individual cells in adult CNS and muscle displayed extreme variations in the amount of transgene transcribed, ranging from undetectable to highly deregulated transcription in neighboring cells. Since very few cells were found to express intermediate levels of HFV, we conclude that transcription, once resumed, rapidly reached maximal levels. The observed distribution suggests that transcription is resumed asynchronously in individual cells. Permanent structural damage was identified only in the striated muscle and in the CNS.

The advanced stages of the disease were characterized by a widespread pathology of the CNS and subtotal necrosis of specific structures such as the hippocampus (Bothe et al., 1991). In addition, animals from two independent families showed prominent cerebellar symptoms due to selective nerve cell loss in the granule cell layer of the cerebellum (A. Aguzzi et al., unpublished data). In the final stages of the disease, total levels of expression in the CNS, as measured by Northern blot analysis, decreased again. It is likely that this apparent decrease reflected degeneration of affected cells.

HFV Toxicity Is Restricted to Adult CNS and Striated Muscle

Although the expression of HFV genes in the embryos appeared to be well tolerated and did not lead to permanent structural damage, it is conceivable that cytotoxicity may have been masked to some extent by the naturally ongoing programmed cell death and by the regenerative capacity of affected systems. However, we infer that this did not occur on a significant scale, since the density of cells undergoing apoptosis in structures expressing the transgene (for example, the dorsal root ganglia and the heart) was not grossly enhanced in comparison with sections of nontransgenic time-matched embryos.

Why are embryonic cells not adversely affected by expression of HFV? Since embryonic expression levels were much lower than those observed in adult diseased organs, it is likely that a threshold of expression must be reached to induce pathological changes, and that the levels of expression during embryogenesis were not sufficient to be toxic. In contrast, adult adipose tissue and smooth musculature did not develop a pathological phenotype despite high levels of expression in single cells. The absence of a pathological phenotype in these tissues may be explained by the much smaller fraction of affected cells and by their higher regenerative potential compared to CNS and striated muscle. However, it is also possible that these cells lack molecular targets for toxicity, or that differential translation of HFV genes in specific tissues does not allow formation of toxic products.

How Can Differential Expression in Embryos and Adult Mice be Explained?

The uneven distribution of cells transcribing HFV in adult mice could suggest a horizontal spread of infectious HFV within affected organs, that is, through a murine helper virus or a replication-competent revertant virus. This seems unlikely, since we did not detect additional HFV integration sites in DNA from adult brain when compared to unaffected tissues in Southern hybridization analyses, and we were unable to demonstrate reverse transcriptase activity in brain preparations of transgenic mice (K. Bothe, unpublished results). Also, the pattern of expression we observed seemed to be independent of the integration site and copy number of the transgene, since it was reproducibly found in mice from independent transgenic families.

It is conceivable that the pattern of expression is dependent on the function of *bcl-1*, the trans-activating

Figure 5. Expression of HFV in histogenetically unrelated organs.

(**a** and **b**) Sagittal sections of the lower abdomen of a 16.5-day-old transgenic embryo. (**c** and **d**) Transverse sections through the pelvis of a newborn transgenic mouse. The positive structures in both sections represent parasympathetic neuroblasts migrating from the remnants of the neural crest toward the myenteric plexus of Auerbach. Ve, vertebral body. (**e** and **f**) Surroundings of Rathke's pouch. The posterior portion of the pituitary gland (neurohypophysis, pp) and the neuroectodermal cells belonging to the basal telencephalon (Ne) display high levels of HFV expression. (**g** and **h**) Sagittal section showing the proximal third of the esophagus (E) in a 16.5-day-old transgenic embryo. Groups of small, tightly packed cells ensheathing the esophageal mucosa both ventrally and dorsally show a distinct hybridization signal.

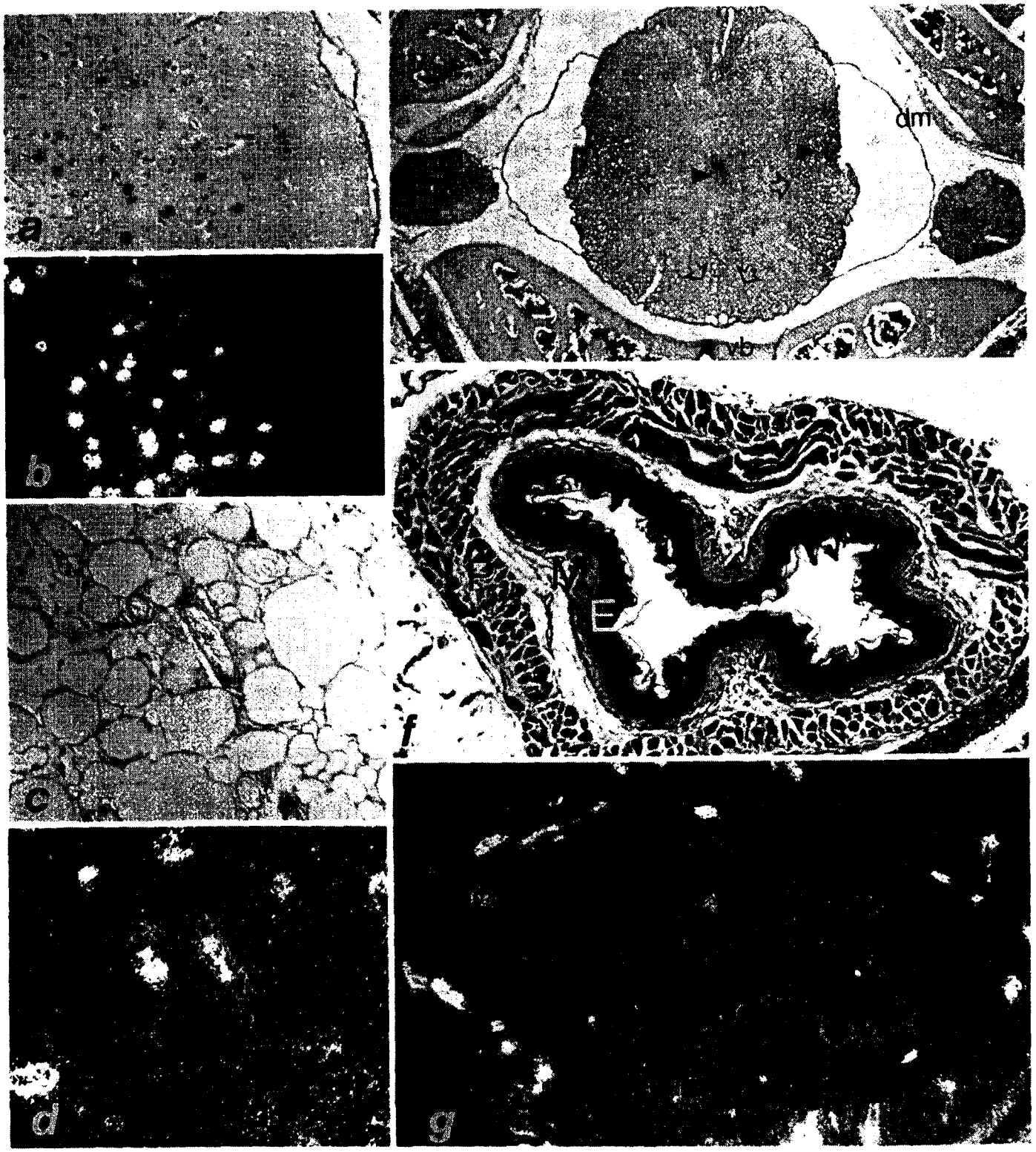

Figure 6. Expression of HFV in adult mice.

In contrast to the embryonic patterns of expression, only a fraction of cells in the respective tissues express the transgene. (**a** and **b**) Expression in the telencephalic cortex of a 5-week-old HFV transgenic mouse is predominantly restricted to a subset of neurons of the pyramidal layer. (**c** and **d**) Expression in adipocytes of the kidney capsule. The bright area within a blood vessel (asterisk) is due to the birefringence of erythrocytes and does not represent a true hybridization signal. Note that the endothelial cells surrounding the blood vessel are negative for HFV expression. (**e**) Cross section through the lower thoracic segment of the spine of a 12-week-old transgenic mouse. Expression is completely abolished in the dorsal root ganglia (drg) and in most cells of the spinal cord. Only few scattered cells in the spinal cord express very high levels of the transgene (arrowheads). Although the gray matter of the spinal cord is basically unaffected, the anterior and lateral tracts of the spinal white matter (open arrows) show severe vacuolar degeneration. dm, dura mater; vb, vertebral body (anterior portion of the vertebra). (**f** and **g**) High levels of expression in randomly distributed smooth and striated muscle cells in the tunica muscularis mucosae (M) and muscularis propria (P) of the esophagus. E, epithelium.

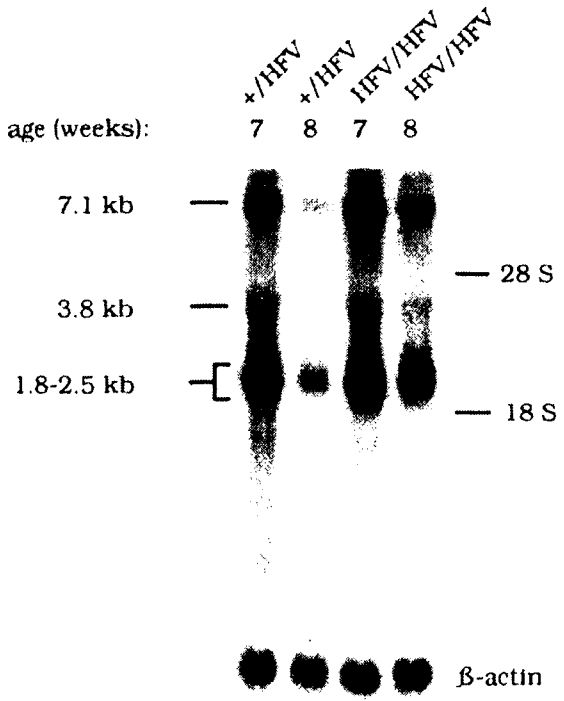

Figure 7. Northern hybridization analysis of brain tissue from heterozygous and homozygous adult animals carrying the pΔgpe transgene.

Left two lanes: Heterozygous mice at 7 and 8 weeks of age. Right two lanes: Homozygous mice at 7 and 8 weeks of age. The weaker signals at 8 weeks of age reflect progressive degeneration of cells expressing HFV, which is characteristic of the final stages of the disease. The 7.1-kb genomic mRNA and the weaker 3.8-kb subgenomic *env* transcript are easily recognizable. The broad band of 1.8 to 2.5 kb represents a group of singly and multiply spliced mRNAs from which the *bel* genes are translated. Heterozygous and homozygous mice do not display significant differences in pattern and intensity of transcription of the transgene. As shown in the lower panel, the amount of RNA loaded has been quantitated by rehybridization of the filter with a β-actin probe.

factor encoded by HFV (Rethwilm et al., 1991). The irregular distribution and asynchronous character of transcriptional activation suggests that stochastically achieved threshold levels of *bel-1* may trigger an irreversible positive feedback loop in individual cells leading to higher transcriptional activity and, in turn, to further accumulation of *bel-1*. The pattern of transgene expression that ultimately resulted may interfere with normal cellular processes and induce cytotoxicity.

In contrast to fully differentiated neural cells, embryonic cells do not allow high levels of HFV expression, suggesting that they are protected from irreversible deregulation of transcription. This is reminiscent of the ability of undifferentiated embryonic cells to silence transcription controlled by viral enhancer elements (Jaenisch et al., 1975, Jaenisch 1980, Gorman et al., 1985). Alternatively, since expression of HFV constructs containing a mutationally inactivated *bel-1* is inefficient (Rethwilm et al., 1991), transcriptional repression may rely on disabling *bel-1* translation, for instance, by differential usage of splice sites. In this case the distribution of transcripts in HFV embryos may reflect basal transcription directed by retroviral cis-regulatory elements. Indeed, the onset of HFV transcription in embryos shows some analogies to that of endogenous mouse retroviruses and IAP particles (Norton and Hogan, 1988) and of experimental infection of embryos with retroviral vectors (Savatier et al., 1990). In addition, it is possible that some of the numerous proteins encoded by HFV constitute a transcriptional silencer, as has been discussed for the *nef* gene product of HIV (Niederman et al., 1989; Cheng-Mayer et al., 1989).

CONCLUSIONS

Although this study has uncovered some unexpected features of the expression of an HFV transgene during development, the molecular basis for these effects is not yet understood. It will be interesting in future studies to determine whether HFV mRNA is

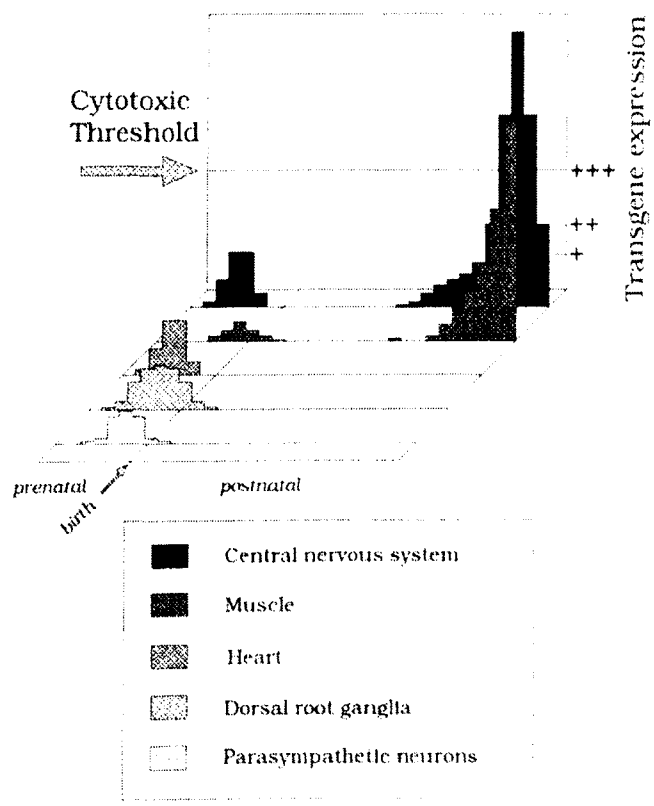

Figure 8. Localization and approximate levels of HFV transgene expression during prenatal and postnatal life.

In situ hybridization analyses were carried out on sections of mice from several independent transgenic families. Although embryonic expression peaked at midgestation or at late gestation in various organ systems, it never reached the high levels seen in adult CNS and muscle. +, Weak signal after 7 days of exposure of hybridized sections; ++, readily visible signal after 7 days but undetectable after 2 days of exposure; +++, signal easily detectable after 1 day of exposure. Cytotoxicity is achieved only when high levels of expression are reached in adult cells belonging to neuroectodermal and myogenic lineages.

differentially processed in embryonic and terminally differentiated neural cells. We are now raising antibodies to the different gene products of HFV that will help us in assessing their respective contributions to the patterns of expression and to the disease. We will also test the effects of different combinations of putative control genes and toxic genes of HFV in transgenic mice. Such studies may provide some insight into the mechanisms underlying HFV-induced disease and, perhaps, into those controlling retroviral latency.

MATERIALS AND METHODS

Construction of HFV Plasmids and Generation of Transgenic Animals

The transgenic mice used in this study contain a linearized form of the plasmid pΔgpe, whose construction has been described by Rethwilm et al. (1991). pΔgpe encodes both long terminal repeats (LTRs) and all regulatory genes of HFV, including the relevant RNA splicing sites, but generation of infectious viral particles is disabled by two deletions in the *gag- pol* and *env* domains (Fig. 1). The derivation and preliminary characterization of transgenic mice is detailed by Bothe et al. (1991).

Collection of Embryonic and Adult Tissues

Heterozygous female transgenic mice were mated to heterozygous males belonging to the same transgenic line. Mating was assumed to occur at midnight: the morning in which a vaginal plug was detected was defined as E0.5 (embryonic day 0.5). Pregnant females were killed at E8.5, E11.5, E13.5, E14.5, and E16.5. Embryos aged 8.5 days were fixed in toto without dissecting them from the uterus: the deciduomas were merely dissected from each other to facilitate infiltration of the fixative through the myometrium, thus preserving the topographic relationship of the fetuses to the extraembryonic tissues. Since fixation of the embryos by this method was not optimal at later time points, older embryos were removed from the uterine cavity and freed from the embryonic membranes prior to fixation. Newborn animals were collected several hours after birth. Additional animals were sacrificed at 3, 5, 8, and 12 weeks of age. Embryos and tissues from newborn and adult mice were fixed in ice-cold paraformaldehyde freshly dissolved in phosphate-buffered saline (4% weight/volume). To speed up infiltration, the abdominal and thoracic cavities, as well as the spinal canal, were exposed prior to submersion in the fixative.

Histopathological Analysis

Conventional histology and further analyses were performed on 35 embryos and 36 mice at various postanatal ages derived from two and eight independent transgenic strains, respectively. Organs were postfixed overnight at 4°C in the solution described above, rinsed briefly with 70% ethanol in diethylpyrocarbonate-treated water, cut into slices of 2 to 3 mm, placed in polyoxymethylene embedding capsules (Semadeni), and dehydrated in a Tissue-Tek automatic infiltrator through an ascending series of RNase-free alcohols and three clearing baths of xylene. Samples were then vacuum-infiltrated with low melting point paraffin (Vogel) at 50°C overnight. The organs of newborn mice containing calcified tissues were decalcified for 72 h with 0.25 M EDTA, pH 7.8. Sections of 3 μm nominal thickness were cut, dried overnight on TESPA-amino-alkylsilane treated slides (Henderson, 1990) at 56°C, deparaffinized in xylene, and either processed for in situ hybridization or stained with hematoxylin and eosin (H&E). Slides were finally dehydrated and mounted in a xylene-compatible medium (Entellan Neu, Merck). All embryos at the age of E8.5 and several selected embryos at later stages were serially sectioned.

In Situ Hybridizations

The transcription vector pG3bel contains an EcoRI-HindIII fragment derived from the *bel* region of HFV (Fig. 1). pG3bel was used to prepare sense and antisense cRNA probes by in vitro transcription in the presence of ^{35}S-rUTP. The radiolabeled transcripts were partially degraded by controlled hydrolysis in 100 mM bicarbonate buffer (pH 9.4, 65°C) to an average length of 50 to 100 bp and resuspended in 50% freshly deionized formamide. The extent of hydrolysis was monitored on a denaturing agarose gel (2% agarose, 10% formaldehyde). In situ hybridizations were performed essentially as described (Aguzzi et al., 1990). Our hybridization mixture contained the radiolabeled probe at a concentration of 200 × 10^3 to 300 × 10^3 dpm/μl in 4× SSC, 50% formamide, 10% dextrane sulfate, 1× Denhard's solution, 100 ng/μl of tRNA, 1 mM unlabeled S-rUTP, and short unrelated unlabeled S-rUTP–containing transcripts in approximately 10× molar excess of the probe. Sense-transcribed RNA probes were used as negative controls. Post-hybridization processing included RNAse A digestion (20 μg/ml, 30 min at 37°C), and several low- and high-stringency washes over a period of 30 h. Slides were then dried, dipped in NTB-2 nuclear track emulsion (Kodak), and exposed at 4°C. The exposure times were 7 to 12 days for embryos, and 1 to 3 days for adult CNS and muscle.

Northern Hybridization Analysis

Total RNA was isolated from brain tissue of 7- and 8-week-old transgenic mice according to standard procedures and separated on 1% denaturing agarose/formaldehyde gels (15 μg/lane), transferred to Genescreen membranes (Amersham), and hybridized to an EcoRI-HindIII fragment of the plasmid pG3bel (see above). This fragment was shown to hybridize to all known HFV transcripts (Figs. 1 and 7). Blots were stripped of radioactivity and rehybridized with a β-actin probe for RNA quantitation.

Photography

Bright-field, dark-field, and differential interference contrast (DIC) photomicrographs were taken on Kodak VPS 135 color daylight negative and on Kodak Tmax black and white films (24 × 36 mm) with a Zeiss Axiophot photomicroscope. Color compensation was achieved with a Kodak 80B filter for bright- and dark-field micrographs and with C10 cyan and Olympus LBT-N filters for DIC. Whenever possible, bright-

field and DIC photographs were taken from H&E-stained serial sections adjacent to those subjected to the hybridization procedure, thereby ensuring optimal staining of cytoplasmic structures and higher contrast of the structures visualized.

Acknowledgments

We are grateful to K. Kratochwil and H. Lassmann for help with reviewing histological sections and for discussions, to H. Haber for technical assistance, and to D.P. Barlow for critical comments. This work was supported by the I.M.P. and by grants of the Deutsche Forschungsgemeinschaft and of the Sander Stiftung to A.R. and to I.H.

REFERENCES

Achong BG, Mansell PW, Epstein MA, Clifford P (1971): An unusual virus in cultures from a human nasopharyngeal carcinoma. J Natl Cancer Inst 46:299-307

Aguzzi A, Wagner EF, Williams RL, Courtneidge SA (1990): Sympathetic hyperplasia and neuroblastomas in transgenic mice expressing polyoma middle T antigen. New Biol 2:533-543

Bothe K, Aguzzi A, Lassmann H, Rethwilm A, Horak I (1991): Progressive encephalopathy and myopathy in transgenic mice expressing human foamy virus genes. Science 253:555-557

Cameron KR, Birchall SM, Moses MA (1978): Isolation of foamy virus from patient with dialysis encephalopathy. Lancet ii:796

Cheng-Mayer C, Iannello P, Shaw K, Luciw PA, Levy JA (1989): Differential effects of *nef* on HIV replication: implications for viral pathogenesis in the host. Science 246:1629-1631

European Collaborative Study (1991): Children born to women with HIV-1 infection: natural history and risk of transmission. Lancet 337:253-260

Coffin J (1990): Retroviridae and their replication. In Fields BN and Knipe DM (eds) Virology, New York, Raven Press, pp 1440-1441

Flügel RM, Rethwilm A, Maurer B, Darai G (1987): Nucleotide sequence analysis of the env gene and its flanking regions of the human spumaretrovirus reveals two novel genes. EMBO J 6:2077-2084

Gallo RC, Wong-Staal F (1990): Retrovirus biology and human disease. New York: Dekker

Giangaspero F, Scanabissi E, Baldacci MC, Betts CM (1989): Massive neuronal destruction in human immunodeficiency virus (HIV) encephalitis. A clinico-pathological study of a pediatric case. Acta Neuropathol (Berl) 78:662-665

Gorman CM, Rigby PWJ, Lane DP (1985): Negative regulation of viral enhancers in undifferentiated embryonic stem cells. Cell 42:519-526

Henderson C (1990): Aminoalkylsilane: an inexpensive, simple preparation for slide adhesion. J Histotechnol 12:123-124

Hinrichs SH, Nerenberg M, Reynolds RK, Khoury G, Jay G (1987): A transgenic mouse model for human neurofibromatosis. Science 237:1340-1343

Jaenisch R, Fan H, Crocker B (1975): Infection of preimplantation mouse embryos and of newborn mice with leukemia virus: tissue distribution of viral DNA and RNA and leukemogenesis in the adult animal. Proc Natl Acad Sci USA 72:4008-4012

Jaenisch R (1980): Retroviruses and embryogenesis: microinjection of moloney leukemia virus into midgestation mouse embryos. Cell 19:181-188

Joshi VV, Oleske JM, Connor EM (1990): Morphologic findings in children with acquired immune deficiency syndrome: pathogenesis and clinical implications. Pediatr Pathol 10:155-165

Kirby ML, Gale TF, Stewart DE (1983): Neural crest cells contribute to normal aorticopulmonary septation. Science 220:1059-1061

Leonard JM, Abramczuk JW, Pezen DS, Rutledge R, Belcher JH, Hakim F, Shearer G, Lamperth L, Travis W, Fredrickson T, Notkins AL, Martin MA (1988): Development of disease and virus recovery in transgenic mice containing HIV proviral DNA. Science 242:1665-1670

Lewis SH, Reynolds-Kohler C, Fox HE, Nelson JA (1990): HIV-1 in trophoblastic and villous Hofbauer cells, and haematological precursors in eight-week fetuses. Lancet 335:565-568

Löchelt M, Zentgraf H, Flügel RM (1991): Construction of an infectious DNA clone of the full length human spumaretrovirus genome and mutagenesis of the bel-1 gene. Virology 184:34-54

Lyman WD, Kress Y, Kure K, Rashbaum WK, Rubinstein A, Soeiro R (1990): Detection of HIV in fetal central nervous system tissue. AIDS 4:917-920

Muller HK, Ball G, Epstein MA, Achong BG, Lenoir G, Levin A (1980): The prevalence of naturally occurring antibodies to human syncytial virus in East African populations. J Gen Virol 47:399-406

Muranyi W, Flugel RM (1991): Analysis of splicing patterns of human spumaretrovirus by polymerase chain reaction reveals complex RNA structures. J Virol 65:727-735

Nerenberg MI, Wiley CA (1989): Degeneration of oxidative muscle fibers in HTLV-1 tax transgenic mice. Am J Pathol 135:1025-1033

Niederman TMJ, Thielan BJ, Ratner L (1989): Human immunodeficiency virus type 1 negative factor is a transcriptional silencer. Proc Natl Acad Sci USA 86:1128-1132

Norton JD, Hogan BLM (1988) Temporal and tissue-specific distribution of distinct retrovirus-like (VL30) elements during mouse development. Dev Biol 125:226-228

Rethwilm A, Mori K, Maurer B, ter Meulen V (1990): Transacting transcriptional activation of human spumaretrovirus LTR in infected cells. Virology 175:568-571

Rethwilm A, Erlwein O, Baunach G, Maurer B, ter Meulen V (1991): The transcriptional transactivator of human foamy virus maps to the *bel 1* genomic region. Proc Natl Acad Sci USA 88:941-945

Savatier P, Morgenstern J, Beddington RSP (1990): Permissiveness to murine leukemia virus expression during preimplantation and early postimplantation mouse development. Development 109:655-665

Stancek D, Stancekova-Gressnerova M, Janotka M, Hnilica P, Oravec D (1975): Isolation and some serological and epidemiological data on the viruses recovered from patients with subacute thyroiditis de Quervain. Med Microbiol Immunol (Berl) 161:133-144

Theiler K (1989): The House Mouse. New York, Springer, ed 2

Werner J, Gelderblom H (1979): Isolation of foamy virus from patients with de Quervain thyroiditis. Lancet ii:258-259